SAND2020-7210C

Exploratory Modeling of Radiation-Induced Photocurrent Response in Vertical GaN Diodes

Presenter:
Matthew J. Jasica
Sandia National Laboratories
Albuquerque, NM
505-284-2115, mjjasic@sandia.gov

Authors:
M. J. Jasica, Sandia National Laboratories[1], 505-284-2115, mjjasic@sandia.gov
W. R. Wampler, Sandia National Laboratories[1], 505-844-4114, wrwampl@sandia.gov
B. Doyle, Sandia National Laboratories[1], 505-844-7568, bldoyle@sandia.gov
G. Vizkelethy, Sandia National Laboratories[1], 505-284-3120, gvizkel@sandia.gov
G. Pickrell, Sandia National Laboratories[1], 505-284-8572, gpickre@sandia.gov
W. Cowan, Sandia National Laboratories[1], 505-844-9379, wdcowan@sandia.gov
A. Colon, Sandia National Laboratories[1], 505-284-6479, acolon@sandia.gov
E. Bielejec, Sandia National Laboratories[1], 505.284.9526, esbiele@sandia.gov

[1]All authors Sandia National Laboratories, Albuquerque, NM

Classification level of final paper and presentation (Unclassified Unlimited Release)
Approved for unlimited release: SAND2019-11359 A

Session and Presentation Preference (Modeling and Simulation, Oral)

Sponsor: DOE NNSA

Abstract (35 words or less)

Photocurrent generation and breakdown in GaN vertical diodes is examined using an exploratory physics model developed at the Sandia Ion Beam Lab. The model is compared to devices exposed to experiments on an electron beam.

Sandia National Laboratories is a multimission laboratory managed and operated by National Technology and Engineering Solutions of Sandia, LLC, a wholly owned subsidiary of Honeywell International, Inc., for the U.S. Department of Energy's National Nuclear Security Administration under contract DE-NA0003525.

EXPLORATORY MODELING OF RADIATION-INDUCED PHOTOCURRENT RESPONSE IN VERTICAL GAN DIODES

Matthew J. Jasica, William R. Wampler, Barney L. Doyle, Georgy Vizkelethy, Gregory W. Pickrell, William Cowan, Albert Colon, Edward Bielejec

I. INTRODUCTION

Gallium nitride (GaN) semiconducting devices are being considered for power electronics operating in radiation environments. Favorable properties include its large band gap (3.4 eV at room temperature), high displacement energy, and large critical electric field (ranging 3 -5 MV-cm^{-1}) [1-3]. Power diodes with breakdown voltages above 3.9 keV and on resistances of 1-2 mΩ-cm^2 have been developed [4, 5]. Radiation can also generate photocurrents in the material from ionizing energy loss (IEL). Under high bias where there are high electric fields in the device, these pulses can trigger avalanches and result in damaging currents to the device. GaN power diodes have also has demonstrated degradation due to displacement damage from either heavy ions or neutrons [6], underscoring the need for better understanding defect physics in GaN.

A 1D exploratory physics development (XPD) model for examining carrier physics and carrier-defect interactions of GaN vertical diodes in radiation environments is being developed at the Sandia National Laboratories Ion Beam Lab. Similar XPD models have been successfully applied towards for GaAs heterojunction bipolar transistors [7, 8] and silicon bipolar junction transistors [9]. As an exploratory model, precise agreement with any specific device is not the primary objective. Rather, the priority is on the identification of key governing physics, primarily those related to defects and carrier-defect interactions that are not addressed in as much detail in commercial Technology Computer-Aided Design (TCAD) software, to replicate device trends in combined environments to better inform to more precise, higher-dimension device or circuit models. Still, it is important to validate the model's performance against actual devices in radiation environments to guide parameter selection and identify potentially missing physics or the limitations of the modeling approach (such as a single dimension). The model development is presently still in the early stages of development. This work focuses on benchmarking the model's performance against baseline power diodes and diode response to photocurrent pulses from gammas or electrons.

II. MODEL

The model tracks the concentrations of six species, versus depth and time, through the modeled device—electrons and holes, a generic defect with three charge states -1, neutral, and +1, and the concentration of ionized acceptors in the p-layer. Carrier transport is modeled by solving the 1D drift-diffusion continuity equations. The chemical potentials for carriers are evaluated using Fermi-Dirac statistics, and include both drift and diffusion terms. Physical processes and reactions for impact ionization and high-voltage breakdown, band structure and carrier mobilities, recombination via Shockley-Reed-Hall (SRH), direct, or Auger emission, partial ionization of acceptors, and carrier generation from ionizing dose rate are included. The local electric potential φ is determined from Poisson's Equation and the net charge density from all carriers, dopants, and charged defect states. The reaction terms are time derivatives of concentrations of the various species due to mechanisms other than drift and diffusion, such as capture and emission of carriers by defects, carrier recombination by band-to-band or defect-assisted processes, and carrier generation from ionizing radiation and impact ionization. Carriers may also move between bands and defect states via band-to-trap tunneling (BTT) in high electric field conditions. The model allows for various doping, geometry, material parameters, and reaction coefficients to be adjusted, depending on the need of the model.

The detailed treatment of carrier-defect interactions, which affect the generation and recombination terms of the drift-diffusion equations, distinguishes this model from commercial TCAD software. These defects may be intrinsic to the device or the result of displacement damage, and may be uniform or have a spatial dependence. The three defect charge state populations (+1, 0, -1) are governed by carrier capture or emission interactions. Defects are allowed to move between charge states via single-carrier interactions, e.g. a neutral defect may capture an electron to transition to a -1 charge state. In this work we use carrier emission/capture energies equal to half the bandgap to represent deep levels, which has the effect that carrier-defect reactions are dominated by carrier capture and BTT, rather than thermal emission. However, this energy level can be adjusted to model specific traps. Dependence of carrier capture rates on temperature and field are included through a multi-phonon emission model for carrier capture and emission [10]. Depth profiles of carrier and defect concentrations, carrier fluxes, and electrical properties such as charge density, field, and potential are tracked to provide a more fundamental understanding of the device physics. The operating parameters of the model may be adjusted to examine device response at different points in time, test different bias regimes or radiation dose rates. An example of the defect population profile using the power diode discussed in Section III is shown in Figure 1.

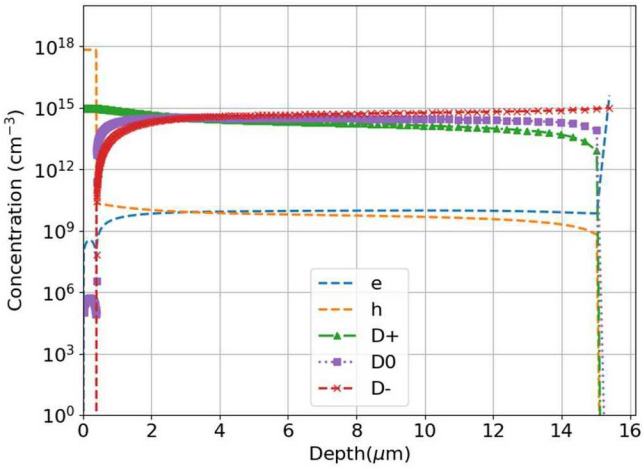

Fig. 1. Example of defect concentration profile as a function of depth is shown for the power diode discussed in Section III with a defect population of 10^{-15} cm^{-3}, biased to -1500 V, and exposed to a dose rate of 4 Mrad/s.

III. EXPERIMENT

The vertical GaN p-n diodes studied for this experiment were grown on n-type, GaN hydride vapor phase epitaxy (HVPE) substrates using metal-organic, chemical vapor deposition (MOCVD). The n-doped layer is 15 µm thick with ~5 × 10^{15} cm^{-3} Si and C donors. The p-type layer is 400 nm thick with doped with 3 × 10^{19} Mg/cm^{3} to give a hole concentration of ~5 × 10^{17} cm^{-3} in the neutral region due to the partial ionization of the acceptors. The devices evaluated have anode contacts of 150 µm or 750 µm diameter and are capped with a 1 µm thick Au contact. Individual devices were separated, packaged, and potted with epoxy to prevent surface breakdown in air.

Packaged devices without potting were exposed to an electron beam to induce photocurrent and simulate Compton electron generation from a gamma environment. Exposures took place in a vacuum chamber with high voltage and current feedthroughs for active device testing. A Keysight B1505A power device analyzer with a high voltage source measurement unit was used to bias the device and measure I-V curves during

the exposure as functions of bias or dose. Diodes were slowly ramped from 0 V until compliance current limits were reached. These limits were set at 1 mA for reverse-bias tests and 8 mA for forward bias tests due to instrument limitations. During this ramp, diodes were irradiated with pulses of 70 keV electrons from an electron gun at various currents (i.e. dose rates), measured using a Faraday cup. Electron pulses were 26 ms in length pulsed at a rate of 2 Hz, to allow for sufficient relaxation of the current to unexposed levels between pulses. Data points taken during pulses were extracted to compose I-V curves under photocurrent exposure. The presence of the Au overlayer reduces the deposited energy in the device by a factor of nearly 0.39 as calculated by PENELOPE [11] a Monte-Carlo electron transport code. The carrier generation rate is obtained by dividing the absorbed ionizing dose rate by 10 eV required to generate an electron-hole pair in GaN.

IV. RESULTS

IV.A. Baseline Performance

The modeled power diodes are reduced to a 1-D p-n junction, ignoring sublayers and accounting for energy loss through overlayers. The 1-D calculation is justified by a diode diameter much greater than its thickness, which should reduce the impact of 2-D structures, such as edge terminations, in the actual diodes. In the absence of data about the spatial defect profile in these devices, a uniform defect distribution of 10^{15} cm^{-3} is assumed for the model. The model is first validated against I-V curves of unexposed devices. Fig. 2 compares model and measured I-V curves for forward-biased devices, with and without defects included in the model. With the proper selection of carrier capture parameters, good agreement is shown at lower biases and currents, where ideal-diode behavior dominates. As current increases and enters a regime where high-carrier injection creates deviation from the ideal diode behavior, divergence of the simulation from the device is observed. Small variation in the turn-on voltage is observed between experiment (2.9 V) and simulation (2.8 V). At higher voltages, a series resistance effect dominates, which is included in the simulation but whose value must be determined empirically.

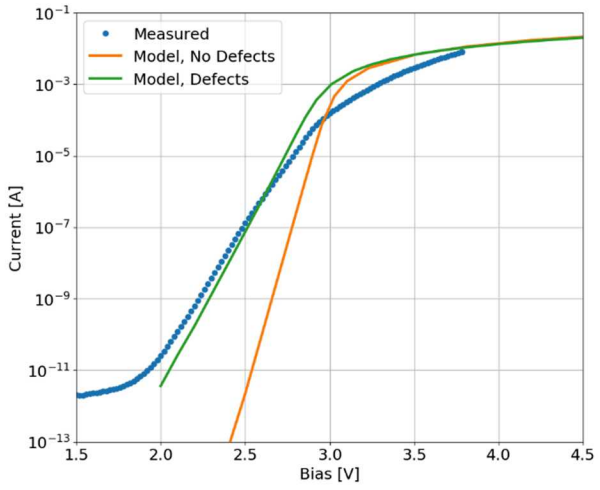

Fig. 2. Forward bias baseline for the 150 μm device, including a 60 Ω series resistance

Baseline comparisons between the experiment and model for the 150 μm diode under reverse bias are shown in Fig. 3. Model configurations without defects, with defects and without BTT, and with defects and BTT are shown. Without BTT, the modeled breakdown voltage overpredicts the device breakdown voltage at 2100 V. A systemic overprediction is expected for this 1D modeling approach, as actual structures produce

concentrated electric fields at edges and reduce the breakdown voltage. Impact ionization is modeled using Chynoweth's equation [12] and parameters adapted from Cao [13] and Dickerson [14]. Small adjustments of these parameters, particularly for the holes, can affect the breakdown voltage. The variation in reported values for impact ionization coefficients [13-15] translates to large variation in breakdown voltage in simulations.

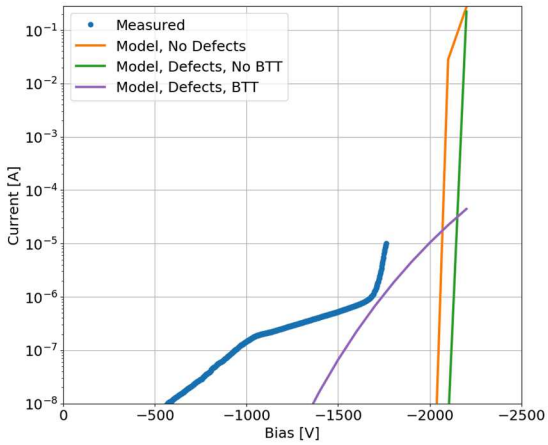

Fig. 3. Reverse-biased I-V curves comparing the measured diode and the model performance with and without defects or band-trap-tunneling (BTT).

The leakage current below breakdown is not accurately modeled in the simulations without BTT, regardless of the treatment of intrinsic defect concentrations or for different energy levels of the modeled trap. A single, generic defect state may not be sufficient to replicate the leakage current. The significance of BTT to leakage current, particularly in the presences of high electric fields is evinced by Fig. 3. The absolute value of the leakage current can be adjusted depending on the selection of material parameters for the multi-phonon emission model. For this work, a phonon energy of 55 meV and a Huang-Rhys factor of 5 were used. Inaccuracy in the absolute reverse leakage current may also suggest incomplete physics or may be a consequence of modeling in 1D. Again, the diode behavior is not expected to be exactly modeled by the XPD model; rather, the goal is to properly capture trends due to the underlaying defect physics.

One unexpected consequence of including BTT in the model is the loss of breakdown under the simulated conditions. This means that under these conditions, the user must choose between investigating leakage current or breakdown effects. Investigations into this behavior are ongoing, but preliminary results suggest that the high trap density used for this work may inhibit a breakdown response in the diode.

IV.B. Photocurrent Response

The I-V curves of 150 µm, and 750 µm devices exposed to the electron beam are shown in Figures 4 and 5, respectively. Two current regimes are observed in the experimental data. At lower biases, the photocurrent scales with dose rate and with the square root of the bias (or the as the width of the depleted region), as expected [16]. While the charge deposition profile of the electron beam varies in space, a uniform radiation profile was applied to the model for simplicity. Band-trap tunneling was disabled for the radiation simulations to investigate breakdown behavior. The primary effect of this is the loss of leakage current in the model. As the photocurrent is at least an order of magnitude larger than the diode leakage current, this approach was deemed to have a minimal impact on the radiation-based calculations.

Strong agreement, within a factor of 2, is observed between the model and experiment across three decades of radiation dose rates for both the 150 µm and 750 µm devices in the classical photocurrent regime at the lower bias, justifying the uniform radiation profile. As the dose rate increases, the onset of charge carrier multiplication occurs in the experimental devices at much lower biases (~700 V or lower) as compared to the unirradiated devices (~1700 V). Some of the experimental data sets suggest this multiplication tapers off as the current approaches 1 mA and reaches a stable regime. However, this is not observed for all sets due to the compliance current limits of 1 mA of the parameter analyzer. This enhanced multiplication regime is not observed in the model, suggesting a limitation of the existing physics in the model.

One open question is the multiplication mechanism governing the dose rate-dependent photocurrent at higher biases. Impact ionization is a well-known mechanism for breakdown in GaN devices [17]. An alternative mechanism is space charge limited current (SCLC), also previously observed in GaN[18], where the filling of both acceptor and donor traps with increasing bias alters the carrier conduction characteristics of the device. One distinguishing characteristic between the two mechanisms is that impact ionization exhibits a temperature dependence while SCLC does not [18]. Experiments on the same experimental setup discussed that probe the temperature dependence of the photocurrent would identify whether this mechanism is responsible for the multiplication regimes observed in Figures 4 and 5.

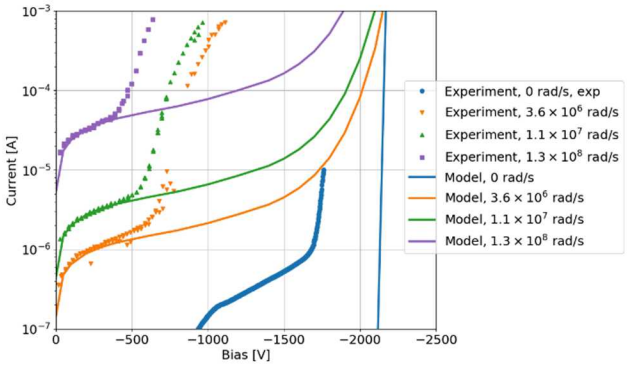

Fig. 4 Reverse biased I-V curves for both model and measurements of the 150 µm device.

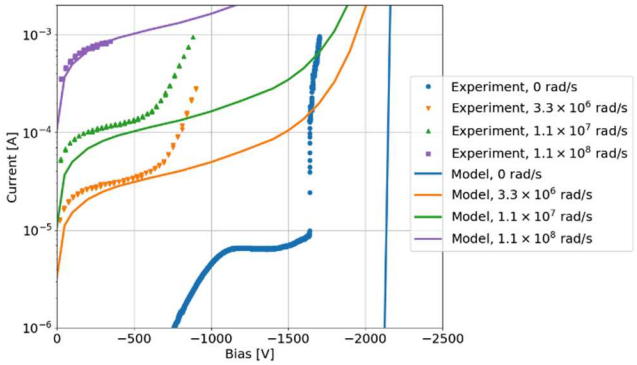

Fig. 5 Reverse biased I-V curves for both model and measurements of the 750 µm device.

REFERENCES

[1] S. J. Pearton, R. Deist, F. Ren, L. Liu, A. Y. Polyakov, and J. Kim, "Review of radiation damage in GaN-based materials and devices," *Journal of Vacuum Science & Technology A: Vacuum, Surfaces, and Films,* vol. 31, no. 5, p. 050801, 2013.

[2] I. Vurgaftman and J. Meyer, "Electron Bandstructure Parameters," in *Nitride Semiconductor Devices: Principles and Simulation*, J. Piprek, Ed.: Wiley, 2007, pp. 13-48.

[3] G. Sabui, P. J. Parbrook, M. Arredondo-Arechavala, and Z. J. Shen, "Modeling and simulation of bulk gallium nitride power semiconductor devices," *AIP Advances,* vol. 6, no. 5, p. 055006, 2016.

[4] I. C. Kizilyalli, T. Prunty, and O. Aktas, "4-kV and 2.8-m Omega-cm(2) Vertical GaN p-n Diodes With Low Leakage Currents," (in English), *Ieee Electron Device Letters,* Article vol. 36, no. 10, pp. 1073-1075, Oct 2015.

[5] A. M. Armstrong *et al.*, "High voltage and high current density vertical GaN power diodes," (in English), *Electronics Letters,* Article vol. 52, no. 13, pp. 1170-1171, Jun 2016.

[6] M. P. King *et al.*, "Performance and Breakdown Characteristics of Irradiated Vertical Power GaN P-i-N Diodes," *IEEE Transactions on Nuclear Science,* vol. 62, no. 6, pp. 2912-2918, 2015.

[7] S. M. Myers, W. R. Wampler, and N. A. Modine, "Recombination by band-to-defect tunneling near semiconductor heterojunctions: A theoretical model," *Journal of Applied Physics,* vol. 120, no. 13, 2016.

[8] W. R. Wampler and S. M. Myers, "Model for transport and reaction of defects and carriers within displacement cascades in gallium arsenide," *Journal of Applied Physics,* vol. 117, no. 4, p. 045707, 2015.

[9] S. Myers, P. Cooper, and W. Wampler, "Model of defect reactions and the influence of clustering in pulse-neutron-irradiated Si," *Journal of Applied Physics,* vol. 104, no. 4, p. 044507, 2008.

[10] R. M. Fleming, S. M. Myers, W. R. Wampler, D. V. Lang, C. H. Seager, and J. M. Campbell, "Field dependent emission rates in radiation damaged GaAs," (in English), *Journal of Applied Physics,* Article vol. 116, no. 1, p. 7, Jul 2014, Art. no. 013710.

[11] F. Salvat, J. M. Fernández-Varea, and J. Sempau, "PENELOPE-2008: A code system for Monte Carlo simulation of electron and photon transport," in *Workshop Proceedings*, 2006, vol. 4, no. 6222, p. 7.

[12] A. G. Chynoweth, "Ionization Rates for Electrons and Holes in Silicon," *Physical Review,* vol. 109, no. 5, pp. 1537-1540, 1958.

[13] L. Cao *et al.*, "Experimental characterization of impact ionization coefficients for electrons and holes in GaN grown on bulk GaN substrates," *Applied Physics Letters,* vol. 112, no. 26, p. 262103, 2018.

[14] J. R. Dickerson *et al.*, "Vertical GaN power diodes with a bilayer edge termination," *IEEE Transactions on Electron Devices,* vol. 63, no. 1, pp. 419-425, 2015.

[15] B. J. Baliga, "Gallium nitride devices for power electronic applications," *Semiconductor Science and Technology,* vol. 28, no. 7, 2013.

[16] S. M. Sze and K. K. Ng, *Physics of semiconductor devices*. John wiley & sons, 2006.

[17] I. C. Kizilyalli, A. P. Edwards, H. Nie, D. Disney, and D. Bour, "High Voltage Vertical GaN p-n Diodes With Avalanche Capability," *IEEE Transactions on Electron Devices,* vol. 60, no. 10, pp. 3067-3070, 2013.

[18] C. Zhou, Q. Jiang, S. Huang, and K. J. Chen, "Vertical Leakage/Breakdown Mechanisms in AlGaN/GaN-on-Si Devices," *IEEE Electron Device Letters,* vol. 33, no. 8, pp. 1132-1134, 2012.